QUASI-ELASTIC LIGHT SCATTERING STUDIES OF MEMBRANE MOTION IN SINGLE RED BLOOD CELLS

ROY B. TISHLER AND FRANCIS D. CARLSON
The Thomas C. Jenkins Department of Biophysics, Johns Hopkins University, Baltimore, Maryland 21218

ABSTRACT Studies of red blood cells (RBCs) and RBC ghosts, using a quasi-elastic light scattering (QELS) microscope spectrometer, have identified the membrane as the primary source of the light scattering signal. This is the first report in which motion of the cell membrane has been demonstrated to be the primary source of the QELS signal from a cell. Cytoplasmic changes induced in the RBC by varying the osmotic strength of the medium were also detected using this technique. Comparison of the data from white blood cells (WBCs) with the RBC data demonstrated significant differences between different types of cells.

INTRODUCTION

QELS has been used to study a wide range of biological problems, including the dynamic properties of intact cells (1). The studies of intact cells have focused on cytoplasmic properties (2) and/or movement of intracellular structures (3, 4). This report describes QELS studies of the membrane[1] in human RBCs.

The QELS technique analyzes the temporal intensity fluctuations of scattered light to obtain information on the dynamic properties of a sample. The fluctuations are characterized by the normalized intensity autocorrelation function, $g^{(2)}(\tau)$, which is defined as (5):

$$g^{(2)}(\tau) = \langle I(t)I(t + \tau)\rangle/\langle I(t)\rangle^2, \qquad (1)$$

where $I(t)$ is the instantaneous intensity the angle brackets indicate the time average, and τ is the delay time. For a monodisperse dilute solution of either freely diffusing isotropic spheres or particles small compared with the wavelength of light, $g^{(2)}(\tau)$ has the form:

$$g^{(2)}(\tau) = 1 + A \exp(-\tau/T_{corr}), \qquad (2)$$

where A is an instrumental constant and T_{corr} is the correlation time of the intensity fluctuations (5). For diffusing particles the intensity fluctuations arise from translational diffusive motion and enable one to determine the diffusion coefficient. The relationship between T_{corr} and the translational diffusion coefficient of the particle, D_T, is:

$$T_{corr} = \tfrac{1}{2}D_T q^2, \qquad (3)$$

where $q = (4\pi/\lambda) \sin(\theta/2)$ is the scattering vector, θ is the scattering angle, and λ is the wavelength of the laser light in solution (5). Using the Stokes–Einstein relationship, D_T can be related to an equivalent hydrodynamic radius, r, by:

$$D_T = kT/6\pi\eta r, \qquad (4)$$

where k is Boltzmann's constant, T is the absolute temperature, and η is the viscosity of the solution (5). The key features of the above equations for the purposes of the following discussion are the $\sin^2(\theta/2)$ dependence of T_{corr}, the exponential form of $g^{(2)}(\tau)$, and the relationship between T_{corr}, D_T, and r that can be derived from Eqs. 3 and 4.

METHODS

A schematic of the QELS microscope spectrometer that was used for the RBC studies is shown in Fig. 1 (6). The diameter of the scattering volume was determined by the front aperture and the objective lens. For the experiments described here, a 330-μm front aperture and 250-μm back aperture were used. With this aperture combination, the spread in scattering angles was $\pm 5.5°$ (6). The use of a 40× objective, in combination with the 330-μm front aperture, gave a scattering volume with a circular cross section 8 μm in diameter. The beam diameter at the sample was ~250 μm and illuminated several cells. Light scattered from a single cell was collected by positioning only one cell within the scattering volume. A photon counting photomultiplier and autocorrelator (7) were used to measure $g^{(2)}(\tau)$. For $\theta \leq 42°$ the sample chamber consisted of a microscope slide and coverslip sealed with petroleum jelly and for $\theta > 42°$ a standard (1 cm × 1 cm × 3 cm) optical cuvette lying on its side was used. Experiments were performed at 16°–21°C.

Please send all correspondence to Dr. Tishler.

[1]The term membrane in this paper refers to the membrane-cytoskeleton complex which remains after the hemoglobin is removed from an RBC. In the following discussion it will be clear that we have actually identified the membrane and/or the cytoskeleton as the source of the signal. Future work will attempt to distinguish the separate contributions of the membrane and the cytoskeleton.
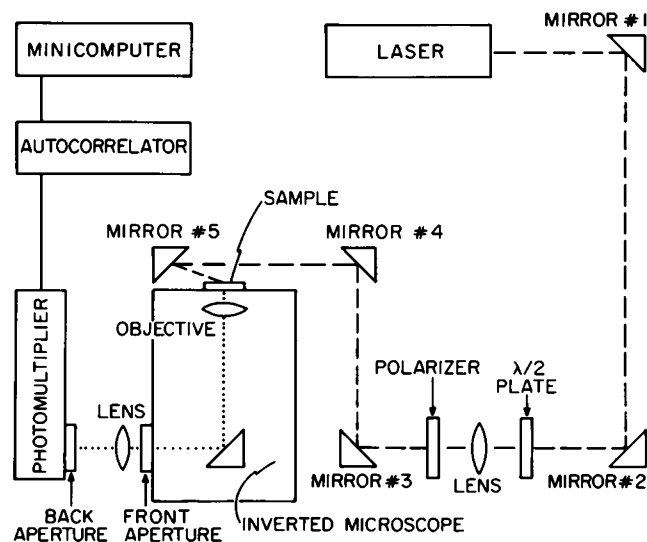
FIGURE 1 Schematic diagram of the QELS microscope spectrometer (6). The system is based on an inverted microscope (Nikon Diaphot). The He-Ne laser beam is directed to the sample by a series of mirrors. Included in the light path are a polarizer and a λ/2 plate to adjust the incident light intensity. The front aperture sets the diameter of the scattering volume and the back aperture the detector area. The scattering angle is set by varying the position of mirror 5. A 40× long-working distance objective is used for all experiments described in this report.

The microscope spectrometer was tested using a model system consisting of a dilute suspension of polystyrene latex spheres. This demonstrated excellent agreement between the theoretical and experimentally determined angular dependence of T_{corr} for θ between 30° and 90° (6).

RBCs were obtained from blood drawn into acid-citrate-dextrose by venipuncture from a 27-yr-old male. The cells were prepared by centrifugation and washed three times in HEPES-Ringers at pH 7.4 (8). Hypertonic buffers were made by the addition of NaCl to the HEPES-Ringers. Modified cells were used within 5 h of preparation. RBC ghosts were prepared using standard techniques (9). WBCs were taken from the "buffy coat" obtained in the initial centrifugation step of a blood preparation and washed as described above for RBCs. All cell preparations were diluted in the buffer in which they were prepared before being placed in the sample chamber. 1 mg/ml bovine serum albumin was added to the dilution buffers.

RESULTS AND DISCUSSION

Typical measurements of $g^{(2)}(\tau)$ obtained from an RBC are shown in Fig. 2. A typical $g^{(2)}(\tau)$ from an RBC ghost is also shown, along with the calculated $g^{(2)}(\tau)$ for a hemoglobin (Hb) solution, based on published QELS values for D_T at high Hb concentrations (10, 11). The autocorrelation function from an RBC using a 40-μs sample time (Fig. 2 A) was similar to that obtained by Nishio et al. from an oxygenated RBC of a person with sickle cell disease (12). Oxygenated sickle RBCs have physical properties similar to the normal adult RBCs studied here, thus the similarity of the results is not surprising. Their calculation gave a correlation length of 300 Å which they interpreted as solely arising from diffusing Hb molecules. In a subsequent study of normal adult RBCs, they included in their analysis a contribution due to motion of the membrane (13). This interpretation agreed more closely with our results.
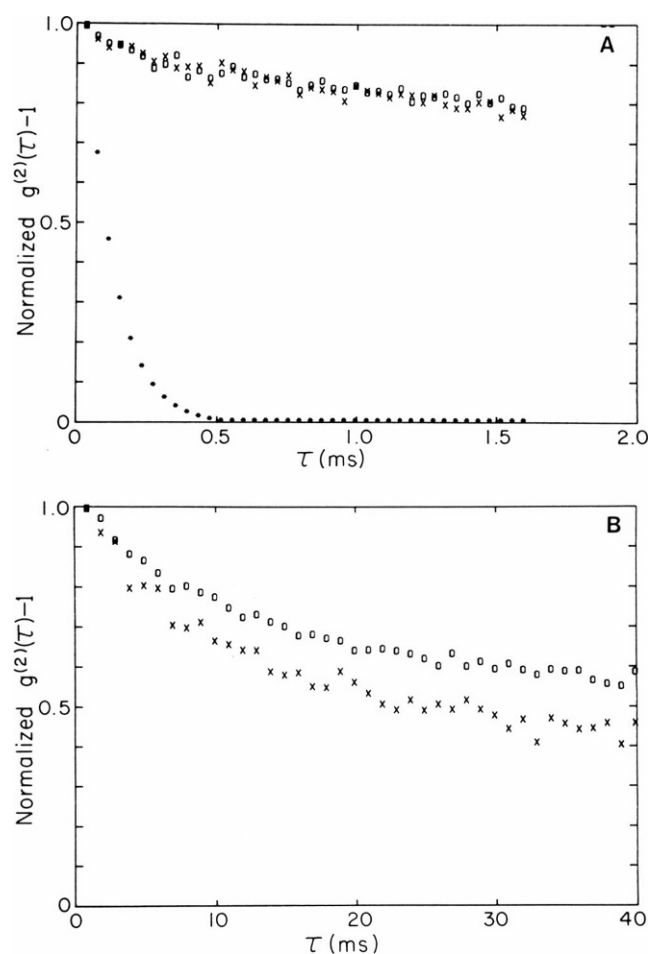

FIGURE 2 $g^{(2)}(\tau)$ measured from a RBC (×), an RBC ghost (O), and $g^{(2)}(\tau)$ calculated for a Hb solution with a concentration of 34 g/dl (*). The $g^{(2)}(\tau)$ calculated for Hb were obtained from QELS measurements made by Jones et al. (10) using their value of D_T and do not account for the second cumulant from a cumulants fit (16). Had this been included, the correlation function for Hb would decay to ~0.1 rather than 0 as depicted in the figure. All data in this and subsequent figures are normalized such that the first point is equal to one. $\theta = 42°$. (A) Sample time 40 μs; (B) sample time 1 ms. (Data for Hb solution is not included in B since only one point would appear on scale near $\tau = 0$.)

The primary source of the QELS signal from an RBC was identified by a comparison of results on the RBC with data from concentrated Hb solutions (10, 11) and RBC ghosts. Hb, which constitutes ~95% of the dry weight of an RBC (14), and the membrane are the two major components of an RBC. If one of these components were the main source of the quasi-elastically scattered light from the RBC, then its measured $g^{(2)}(\tau)$ should be similar to the $g^{(2)}(\tau)$ measured from the intact cell.

Comparison of $g^{(2)}(\tau)$ measured from RBCs with data from concentrated Hb solutions suggested that Hb was not the primary source of the QELS signal from RBCs. QELS determinations of D_T for Hb, extrapolated to infinite dilution (10, 11), yield values for r of ~31 Å, which are in good agreement with values obtained by other methods (15). As the Hb concentration was increased from 0.1 g/dl

TABLE I
QELS STUDIES OF RED BLOOD CELLS USING DIFFERENT SCATTERING ANGLES AND SAMPLE TIMES

	Correlation times (ms)			
	Red blood cells (sample times)			Concentrated Hb
θ_{sc}	10 μs	40 μs	100 μs	calculated
32°	2.9 ± 1.0 (4)	8.5 ± 2.7 (4)	13.8 ± 5.9 (4)	0.175
42°	3.8 ± 1.5 (6)	9.8 ± 4.5 (6)	12.9 ± 3.0 (6)	0.104
65°	3.8 ± 1.1 (7)	7.8 ± 1.4 (7)	13.2 ± 2.8 (7)	0.046
78°	3.9 ± 0.8 (7)	8.4 ± 1.5 (7)	16.3 ± 4.4 (7)	0.034

Measurements from individual RBCs at different scattering angles and sample times. The correlation times were obtained from single exponential fits to $g^{(2)}(\tau) - 1$. Values listed are the mean and standard deviation of (n) cells. The Hb data are based on data from Jones et al. (10). Their value for the translational diffusion coefficient of Hb at a concentration of 34 g/dl (approximately the physiological concentration) was used to calculate the correlation time at a range of angles. This tables shows the following: (a) the QELS signal from individual RBCs is a complicated signal and cannot be described by a single exponential; (b) the value of the correlation time is a strong function of the sample time used; (c) the signal from RBCs is essentially angle independent over a range of scattering angles from 32° to 78°; and (d) the correlation times for Hb are much shorter than those measured for the RBC.

to 37 g/dl, D_T decreased by ~25% (10). If this resulted from a change in the effective size of the molecule, r increased by ~25%. For the most concentrated Hb solutions in which the scattering vector dependence has been studied (19.2 g/dl), D_T exhibited the predicted dependence on q as both θ and λ were varied (11). In addition, Jones et al. (10) noted an increase in the second cumulant (16) of their data analysis for Hb concentrations >20 g/dl. This increase indicates that above 20 g/dl there is an increase in the width of the distribution of D_T values. However, this does not alter the linear relationship between D_T and Hb concentration (10). Even allowing for variations due to the second cumulant, there is still a substantial difference between $g^{(2)}(\tau)$ measured from an RBC and that measured from a concentrated Hb solution (Fig. 2 A).

T_{corr} for the RBCs was calculated by fitting $g^{(2)}(\tau)$ with Eq. 2. The value of T_{corr} was a strong function of the sample time, increasing as longer sample times were used (Table I). These results indicate that $g^{(2)}(\tau)$ for an RBC is not a single exponential but consists of a range of correlation times. Longer correlation times become significant as the sample times increase. However, if T_{corr} obtained using sample times of 10–100 μs were interpreted as arising from diffusing particles, the radii would be 0.07–2.0 μm.[2] This is

---

[2]The analysis presented here assumes homodyne detection (2). Measurements of the amplitude of $g^{(2)}(\tau) - 1$ using polystyrene latex spheres gave values (~0.7) that were in agreement with theory. The low amplitude of $g^{(2)}(\tau) - 1$ for the RBC data (<0.1) had two possible causes: the motion leading to the intensity fluctuations had a small amplitude (17) or (b) heterodyne detection of the scattered light is occurring. If heterodyne detection were taking place, the values for the hydrodynamic radii we calculated would increase by at most a factor of 2. However, the conclusions remain unchanged.

15 to 500 times larger than the diameter of ~40 Å inferred from QELS studies on concentrated Hb solutions (10). If data collected at 32° using a 40-μs sample time are fit with Eq. 2, values of ~0.19 μm are obtained for the particle radius. However, a third order cumulants fit (16) gives a radius of ~400 Å which is comparable to the 300 Å values of Nishio et al. (12) under similar experimental conditions. This value is an order of magnitude higher than that for concentrated Hb. In their later work, Nishio et al. (13) approximated the membrane contribution by a single exponential. The values for the radius of Hb calculated from their measurements of D_T were still two to eight times higher than the values obtained from concentrated Hb solutions (10).

The angular dependence of $g^{(2)}(\tau)$ for $32° < \theta < 78°$ was measured for RBCs using sample times of 10, 40, and 100 μs (Table I). A fivefold change in T_{corr} would be expected if $g^{(2)}(\tau)$ originated from freely diffusing Hb. In fact no angular dependence was detected. This angular independence of $g^{(2)}(\tau)$ from an RBC is inconsistent with the data from concentrated Hb solutions (11).

Light scattering from the membrane of the RBC was studied using RBC ghosts that contained a negligible amount of Hb (9). The intensity of scattered light per unit of incident power from ghosts was approximately 1/10 that from RBCs. This was presumably due to the decreased refractive index gradient between the "cytoplasm" of the ghost (which consists of buffer) and the buffer itself as compared with the relatively large contrast between the cytoplasm of an RBC and the buffer. Measurements on ghosts also demonstrated more variability between individual cells. Despite these differences, the similarity between $g^{(2)}(\tau)$ from an RBC ghost and an RBC is striking (Fig. 2).

Motion of the individual cells was ruled out as the source of the QELS signal by examining RBCs attached to a microscope slide by polylysine. The results were indistin-
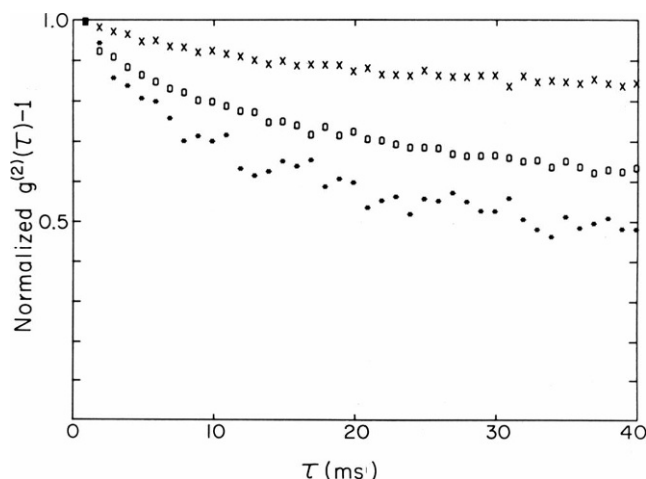

FIGURE 3 Comparison of RBCs in different osmotic strength buffers. Isotonic (*), 2× isotonic (O), and 2.5× isotonic (×). Sample time 1 ms. $\theta = 42°$.

guishable from those shown in Fig. 2 B, where the RBC is resting on the surface of the slide.

The similarity between ghost and RBC data and the discrepancies between $g^{(2)}(\tau)$ obtained from an RBC and concentrated Hb solution support the conclusion that the primary source of the QELS signal from an RBC is the membrane. This result raises the following question: why was there little or no contribution observed from Hb to $g^{(2)}(\tau)$? Possible explanations for this are that the diffusive motion of Hb is restricted intracellularly or that the fluctuating component of the scattered intensity from the membrane is much greater than that due to Hb.

The $g^{(2)}(\tau)$ measured from an RBC was also sensitive to changes in the cell's cytoplasmic properties. When the osmotic strength of the buffer is increased by the addition of NaCl, water leaves the cell and its protein concentration (and cytoplasmic viscosity) is increased (18). Measurements of $g^{(2)}(\tau)$ in increased osmotic strength buffers showed an increase in correlation time, which was due presumably to a damping of the membrane motion by the more viscous cytoplasm (Fig. 3). Cells in a hypoosomotic (50%) HEPES buffer studied at lower scattering angles (33°) showed small, but not statistically significant, increases in correlation times (data not shown). A possible mechanism in this case was increased tension on the membrane due to swelling of the cell.

The similarity between $g^{(2)}(\tau)$ for ghosts and RBCs raised the question of whether the same signal might be seen in other types of cells. The shape of the WBC (polymorphonuclear cell) differs from the RBC and its cytoplasmic viscosity is two to three orders of magnitude higher (19). The measured $g^{(2)}(\tau)$ from the WBC decayed much more slowly than $g^{(2)}(\tau)$ from RBCs (Fig. 4).

The question of what membrane motion of the RBC might lead to the measured intensity fluctuations is particularly interesting since the cell has no known inherent capability for motility. A possible cause of the motion is
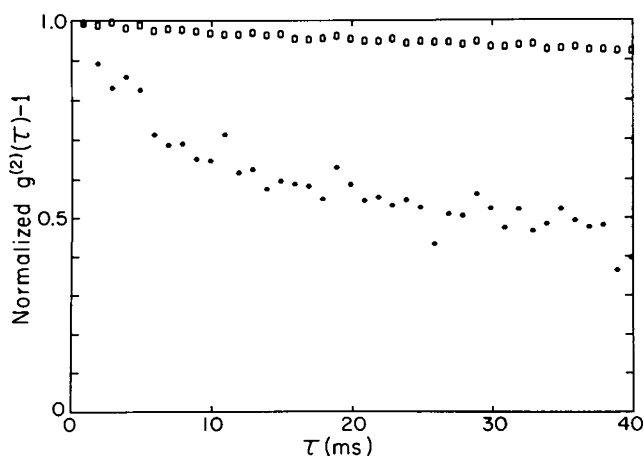
thermal fluctuations of the membrane shape. These fluctuations lead to ripples or waves at fluid interfaces and surfaces. Theoretical and experimental studies of these fluctuations have been made for monolayers (20), vesicles (21, 22), and RBCs (23). The optical manifestations of these fluctuations in the RBC have been cited as the physical basis for the so-called "flicker" phenomenon (23). Flicker has been studied quantitatively using phase microscopy to measure thickness fluctuations of the cell (23). In addition, intensity fluctuations have been noted in experiments measuring the intensity of laser light scattered from RBCs at small angles (24). These fluctuations were an incidental finding in a study of intracellular Hb and have been attributed to flicker. Membrane fluctuations have also been studied in model vesicle systems using video techniques (21, 22). Since our studies involved shorter time scales, different scattering angles, and a different detection scheme than these other studies, a definitive association between thermal fluctuations of the membrane and the intensity fluctuations reported in this work cannot be made.

SUMMARY

Membrane motion in the RBC has been detected by measurements of the intensity autocorrelation function of quasi-elastically scattered laser light. The structural simplicity of the RBC has allowed us, for the first time, to identify the membrane as the source of the intensity fluctuations of quasi-elastically scattered light from a cell. The question of why there is apparently no significant contribution from Hb has been raised.

Future QELS studies of cellular and intracellular phenomena must consider possible membrane effects. For example, in a study of rat adrenals by Englert (25), the slowly decaying nonexponential autocorrelation function was attributed to constrained diffusion of chromaffin granules. The data presented above show that a contribution from the membrane could lead to a similar result.

The QELS technique allows the study of membrane properties of the individual RBCs in a nonperturbing manner, making it ideal for studying changes in the membrane induced by physiological or biochemical means. Changes in the scattered light in response to changes of the cytoplasmic viscosity can also be monitored through indirect effects on the membrane. Future studies will make use of these features and will also relate the QELS information on membrane motion to the data obtained using other techniques.

FIGURE 4 Comparison of RBC (∗) and WBC (O). Sample time 1 ms. $\theta = 42°$.

REFERENCES

1. Earnshaw, J. C., and M. W. Steer, eds. 1983. The application of laser light scattering to the study of biological motion. Plenum Publishing Corp., New York.

2. Sun, S.-T., T. Tanaka, I. Nishio, J. Petermans, J. V. Maizel, Jr., and J. Piatigorsky. 1984. Direct observation of δ-crystallin accumulation by laser light-scattering spectroscopy in the chicken embryo lens. *Proc. Natl. Acad. Sci. USA.* 81:785–787.

3. Mustacich, R. V., and B. R. Ware. 1976. A study of protoplasmic streaming in the Nitella by laser doppler spectroscopy. *Biophys. J.* 16:373–388.

4. Sattelle, D. B., D. J. Greene, and K. H. Langley. 1979. Subcellular motions in *Nitella flexis* studied by photon correlation spectroscopy. *Physica Scripta.* 19:471–475.

5. Cummins, H. Z., and E. R. Pike, eds. 1974. Photon Correlation and Light Beating Spectroscopy. Plenum Publishing Corp., New York. 285–330, 387–428.

6. Blank, P. S., R. B. Tishler, and F. D. Carlson. 1987. Quais-elastic light scattering microscope spectrometer. *Applied Optics.* 26:351–356.

7. Haskell, R. C., and F. D. Carlson. 1981. Quasi-elastic light scattering studies of single skeletal muscle fibers. *Biophys. J.* 33:39–62.

8. Schindler, M., D. E. Koppel, and M. P. Sheetz. 1980. Modulation of membrane protein lateral mobility by polyphosphates and polyamines. *Proc. Natl. Acad. Sci. USA.* 77:1457–1461.

9. Lin, S., and C. E. Snyder. 1977. High affinity cytochalasin B binding to red cell membrane proteins which are unrelated to sugar transport. *J. Biol. Chem.* 252:5464–5471.

10. Jones, C. R., C. S. Johnson, and J. T. Penniston. 1978. Photon correlation spectroscopy of hemoglobin: diffusion of Oxy-Hb and Oxy-HbS. *Biopolymers.* 17:1581–1593.

11. Hall, R. S., Y. S. Oh, and C. S. Johnson. 1980. Photon correlation spectroscopy in strongly absorbing and concentrated samples with application to unliganded hemoglobin. *J. Phys. Chem.* 84:756–767.

12. Nishio, I., T. Tanaka, S.-T. Sun, Y. Imanishi, and S. T. Onishi. 1983. Hemoglobin aggregation in single red blood cells of sickle cell anemia. *Science (Wash. DC).* 220:1173–1175.

13. Nishio, I., J. Peetermans, and T. Tanaka. 1985. Microscope laser light scattering spectroscopy of single biological cells. *Cell Biophys.* 7:91–105.

14. Mountcastle, V. B., ed. 1980. Medical Physiology, Vol. II. The C. V. Mosby Co., St. Louis, MO. 1126–1136.

15. Muirhead, H., J. M. Cox, L. Mazzarella, and M. F. Perutz. 1967. Structure and function of haemoglobin III. A three-dimensional Fourier synthesis of human deoxyhaemoglobin at 5.5 Å resolution. *J. Mol. Biol.* 28:117–156.

16. Koppel, D. E. 1972. Analysis of macromolecular polydispersity in intensity correlation spectroscopy: the method of cumulants. *J. Chem. Phys.* 57:4814–4820.

17. Carlson, F. D., and A. B. Fraser. 1974. Dynamics of F-actin and F-actin complexes. *J. Mol. Biol.* 89:273–281.

18. McConaghy, P. D., and M. Maizels. 1961. The osmotic coefficient of haemoglobin in red cells under varying conditions. *J. Physiol. (Lond.).* 155:28–45.

19. Sung, K.-L. P., G. W. Schmid-Schonbein, R. Skalak, G. B. Schuessler, S. Usami, and S. Chien. 1982. Influence of physiochemical factors on rheology of human neutrophils. *Biophys. J.* 39:101–106.

20. Earnshaw, J. R. 1983. Light scattering by model membranes. *In* The application of laser light scattering to the study of biological motion. J. C. Earnshaw and M. W. Steer, editors. Plenum Publishing Corp., New York.

21. Schneider, M. B., J. T. Jenkins, and W. W. Webb. 1984. Thermal fluctuations of large quasi-spherical bimolecular phospholipid vesicles. *J. Phys. (Paris).* 45:1457–1472.

22. Englehardt, H., H. P. Duwe, and E. Sackmann. 1985. Bilayer bending elasticity measured by Fourier analysis of thermally excited undulations of flaccid vesicles. *J. Phys. (Paris).* 46:L395–L400.

23. Brochard, F., and J. F. Lennon. 1975. Frequency spectrums of the flicker phenomenon in erythrocytes. *J. Phys. (Paris).* 36:1035–1047.

24. Colletta, M., J. Hofrichter, F. A. Ferrone, and W. R. Eaton. 1982. Kinetics of sickle haemoglobin polymerization in single red cells. *Nature (Lond.).* 300:194–197.

25. Englert, D. F. 1980. An optical study of isolated rat adrenal chromaffin cells. *Exp. Cell Res.* 125:369–375.